Kinetics and Electron Paramagnetic Resonance Evidence of an Electron-transfer Chain Mechanism for PPh_3 Substitution of $[Fe_3(CO)_{12}]$†

Feng-Hurng Luo, Shehng-Rur Yang, Chen-Shun Li, Jiun-Pey Duan and Chien-Hong Cheng *
Department of Chemistry, National Tsing Hua University, Hsinchu, Taiwan 30043, Republic of China

Rapid PPh_3 substitution of $[Fe_3(CO)_{12}]$ to give $[Fe_3(CO)_{11}(PPh_3)]$ occurs in tetrahydrofuran at ambient temperature. The reaction is independent of the complex concentration. An electron-transfer-catalysed mechanism is operative in this reaction, with $[Fe_3(CO)_{12}]^{\bullet -}$ as the catalytically active species. The EPR studies indicate that $[Fe_3(CO)_{12}]^{\bullet -}$ is produced rapidly at the beginning of the reaction and its concentration is maintained at a constant value during the reaction. The substitution rate is equal to $k[Fe_3(CO)_{12}^{\bullet -}]$ with $k = (2.7 \pm 0.1) \times 10^{-3}$ s^{-1}. Dissociation of a CO ligand from this radical to yield $[Fe_3(CO)_{11}]^{\bullet -}$ is the rate-limiting step for this electron catalysis. It is believed that $[Fe_3(CO)_{12}]^{\bullet -}$ is formed from a fast disproportionation of $[Fe_3(CO)_{12}]$ induced by an impurity in PPh_3. The impurity is likely PPh_3O and its concentration is proportional to that of the PPh_3 used.

Ligand substitutions of organometallic compounds *via* an electron-transfer chain (e.t.c.) mechanism have frequently been observed.[1–11] In general, the key intermediate in these reactions are the corresponding 17- and 19-electron organometallic species which undergo rapid substitution and electron-transfer reactions. The kinetics of these odd-electron complexes has been studied.[12–16] It has now become clear that in most cases a 17-electron radical undergoes substitution *via* an associative pathway. Second-order kinetics, being first order in the concentration of the radical and also in that of the entering group, is observed for this type of replacement reaction.[12–15] In contrast, the substitution reaction of a 19-electron species takes place *via* a dissociative mechanism. The rate of the reaction depends only on the concentration of the radical.[16] Despite the fact that the kinetics and mechanisms involving these odd-electron species have been well established, little is known regarding the kinetics of the related electron-transfer-catalysed substitution reaction which consists of these individual steps and an electron-transfer process.

Previously, we have shown that the reaction of $[Fe_3(CO)_{12}]$ with CO in tetrahydrofuran (thf) to yield $[Fe(CO)_5]$ [equation (1)] also occurs *via* an electron-transfer chain mechanism.[17]

$$[Fe_3(CO)_{12}] + 3CO \longrightarrow 3[Fe(CO)_5] \qquad (1)$$

This cluster degradation is initiated by the disproportionation of $[Fe_3(CO)_{12}]$ to produce the active $[Fe_3(CO)_{12}]^{\bullet -}$. One key step of this electron-catalysed reaction is proposed to be a Fe–Fe bond cleavage of the 19-electron triangular $[Fe_3(CO)_{12}]^{\bullet -}$ to give the 17-electron linear-chain radical anion $[Fe(CO)_4$–$Fe(CO)_4$–$Fe(CO)_4]^{\bullet -}$. The reaction of CO with this linear chain species gives the degradation product $[Fe(CO)_5]$ and $[Fe(CO)_5]^-$. An electron transfer from the latter radical anion to $[Fe_3(CO)_{12}]$ regenerates the active $[Fe_3(CO)_{12}]^{\bullet -}$.

The kinetics and mechanisms of the reaction of $[Fe_3(CO)_{12}]$ with PPh_3 in hydrocarbons have been studied by two groups. Shojaie and Atwood[18] have shown that the phosphine substitution rate in hexane is first order in $[Fe_3(CO)_{12}]$ and independent of $[PPh_3]$. A dissociative pathway was proposed for this substitution. In the other study in benzene, however, the observed rate constant for the reaction is found to be a combination of two terms.[19] Both substitution and fragmentation take place at comparable rates under the reaction conditions [equation (2)]. Related work reported by Basolo and co-

$$k_{obs} = k_1[Fe_3(CO)_{12}] + \{k_2[PPh_3]/[Fe_3(CO)_{12}]\} \qquad (2)$$

workers[20] revealed that the reaction of $[Fe_3(CO)_{12}]$ with PPh_3 in the presence of trimethylamine oxide to give $[Fe_3(CO)_{11}(PPh_3)]$ is first order in $[Fe_3(CO)_{12}]$ and independent of $[PPh_3]$.

The unprecedented electron-transfer mechanism for the degradation of $[Fe_3(CO)_{12}]$ [equation (1)] prompted us to investigate further the reaction of $[Fe_3(CO)_{12}]$ with other ligands. In this paper we examine in depth the substitution of $[Fe_3(CO)_{12}]$ with PPh_3 in thf including kinetic and EPR studies. Surprisingly, the observed kinetics and the mechanism differ dramatically from those in hydrocarbons reported earlier.

Experimental

Iron pentacarbonyl (Strem), triphenylphosphine oxide (Aldrich) and triphenylphosphine (TCI) were used as purchased. Tetrahydrofuran was distilled from sodium/potassium diphenylketyl and stored under argon. Other solvents were of reagent grade, and were dried and degassed before use. The compound $[Fe_3(CO)_{12}]$ was prepared according to the procedure of McFarlane and Wilkinson.[21] The method of Shojaie and Atwood[18] was used to synthesise $[Fe_3(CO)_{11}(PPh_3)]$.

Infrared spectra were recorded on a Perkin-Elmer 580 spectrophotometer, ultraviolet-visible spectral measurements on a Hitachi U-3200 spectrophotometer with 2 mm cells. Electron paramagnetic resonance spectra were obtained on a Brücker 200D SRC spectrometer operated in the X band. The instrument is equipped with an NMR gaussmeter (ER 035M), a microwave frequency counter (Brücker model 371) and a variable-temperature accessory (Brücker ER 4111-VT).

Kinetic Measurements.—The reaction of $[Fe_3(CO)_{12}]$ with PPh_3 in thf was studied at 20 °C. All reactions were carried out under the conditions where the concentration of PPh_3 was at least greater than 10 times that of $[Fe_3(CO)_{12}]$. In a typical kinetic experiment (run 1 in Table 1), two separate flasks containing 0.0263 mol dm^{-3} PPh_3 solution (25.0 cm^3 of thf) and $[Fe_3(CO)_{12}]$ (0.0307 g, 0.61 × 10^{-4} mol) respectively were

† *Non-SI unit employed:* G = 10^{-4} T.

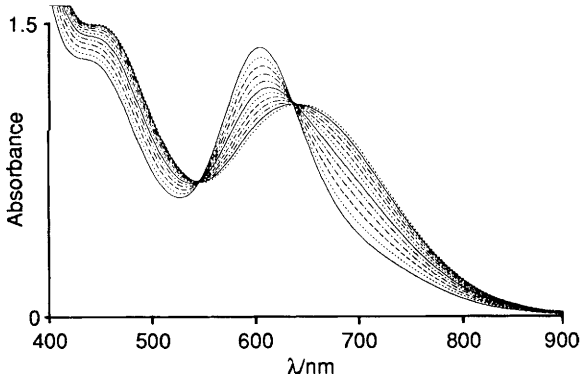

Fig. 1 Ultraviolet–visible spectral changes of a mixture of $[Fe_3(CO)_{12}]$ and PPh_3 in thf as a function of time; the time interval between spectroscopic measurements was 5 min. See run 1 in Table 1 for reaction conditions

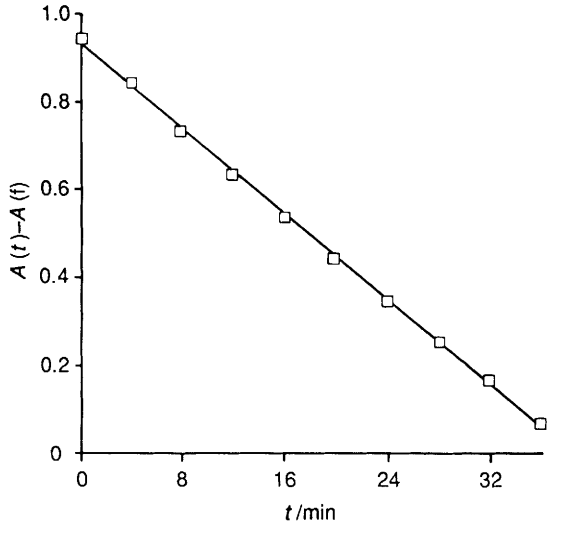

Fig. 2 The absorbance at 600 nm of a mixture of $[Fe_3(CO)_{12}]$ and PPh_3 in thf as a function of time; $[Fe_3(CO)_{12}] = 3.27 \times 10^{-3}$, $[PPh_3] = 6.07 \times 10^{-2}$ mol dm^{-3}, 20 ± 0.1 °C. See text for the definition of $A(t)$ and $A(f)$

Table 1 Effect of the concentration of PPh_3 and $[Fe_3(CO)_{12}]$ on the substitution rate *

Run	10^3 $[Fe_3(CO)_{12}]$/ mol dm^{-3}	10^2 $[PPh_3]$/ mol dm^{-3}	10^6 Rate/ mol dm^{-3} s^{-1}
1	2.44	2.63	0.577
2	2.47	5.21	1.26
3	2.53	7.81	1.75
4	2.48	10.4	2.36
5	2.45	13.0	3.00
6	2.47	15.6	3.67
7	1.64	7.78	1.69
8	3.40	7.79	1.71
9	4.11	7.78	1.77

* In thf at 20 ± 0.1 °C.

placed in an internal circulating bath at 20 ± 0.1 °C. After 30 min of temperature equilibration, the PPh_3 solution (25.0 cm^3) in one flask was syringed into the other flask containing $[Fe_3(CO)_{12}]$ and rigorously shaken. An aliquot (0.8 cm^3) of the solution was quickly withdrawn and injected *via* a septum into a 2 mm cuvette which was placed in a temperature-regulated jacket maintained at 20 °C by the same circulating bath. The reactions were followed by measuring the absorbance at 600 nm as a function of time. Plots of absorbance *vs.* time were linear up to more than 90% completion of reaction.

EPR Measurements.—The solutions for EPR studies were prepared in a way similar to those for kinetic studies. Diphenylpicrylhydrazyl (dpph) was used as an external standard for calculating g values and the relative intensities of EPR signals as the concentration of PPh_3 or $[Fe_3(CO)_{12}]$ varied.

Results and Discussion

Reaction of $[Fe_3(CO)_{12}]$ *with* PPh_3.—To understand the nature of the reaction of $[Fe_3(CO)_{12}]$ with PPh_3 in thf we monitored the solution by ultraviolet–visible spectroscopy. Fig. 1 reveals a typical spectral change in the region 400–900 nm as a function of reaction time. A rapid decrease in intensity of the absorption of $[Fe_3(CO)_{12}]$ at 600 nm is accompanied by a concurrent increase in the absorption band at 660 nm leading to the formation of two isosbestic points at 554 and 640 nm. The band at 660 nm is known to be from $[Fe_3(CO)_{11}(PPh_3)]$,[20] which we verified by comparing it with a spectrum of an authentic sample synthesised by a reported method.[18,22] Thus, the observed change in the spectrum of the $[Fe_3(CO)_{12}]$–PPh_3 solution may be summarized according to equation (3).

$$[Fe_3(CO)_{12}] + PPh_3 \longrightarrow [Fe_3(CO)_{11}(PPh_3)] + CO \quad (3)$$

Further reaction of $[Fe_3(CO)_{11}(PPh_3)]$ with PPh_3 occurred as indicated by the decrease in intensity of the band at 660 nm after $[Fe_3(CO)_{12}]$ disappeared. The final products of this reaction were identified as $[Fe(CO)_4(PPh_3)]$ and $[Fe(CO)_3(PPh_3)_2]$. However, the rate of this fragmentation reaction is much slower, requiring more than 10 h to complete, compared with reaction (3).

Kinetics.—Analysis of the ultraviolet–visible spectra of the $[Fe_3(CO)_{12}]$–PPh_3 solution at different reaction times revealed interesting kinetic results. Plots of $A(t) - A(f)$ *vs.* time were always linear; a typical example is shown in Fig. 2, in which $A(t)$ and $A(f)$ are the absorbances at 600 nm at time t and at the end of substitution, respectively. Because $[Fe_3(CO)_{11}(PPh_3)]$ reacts further with PPh_3 to give mononuclear products after a prolonged reaction time, we assume that $A(f)$ is the absorbance of $[Fe_3(CO)_{11}(PPh_3)]$ whose concentration is the same as that of the initial $[Fe_3(CO)_{12}]$. It should be noted that the linear relationship in Fig. 2 and thus the rate of substitution shown in equation (3) are not affected by the value of $A(f)$ employed. The observed linear plot strongly indicates that the substitution reaction (3) is independent of $[Fe_3(CO)_{12}]$ concentration. These linear plots were obtained for runs with different concentrations of $[Fe_3(CO)_{12}]$ and PPh_3. Careful examination of these plots indicates that a short induction period of less than 2 min is required to start the substitution. From the slopes of these plots and the absorption coefficients of $[Fe_3(CO)_{12}]$ and $[Fe_3(CO)_{11}(PPh_3)]$ at 600 nm (ε_{600} = 2937 and 1416 dm^3 mol^{-1} cm^{-1} respectively) and assuming that all $[Fe_3(CO)_{12}]$ disappeared has been converted into $[Fe_3(CO)_{11}(PPh_3)]$ (see Fig. 1), the rates of the decrease in $[Fe_3(CO)_{12}]$ under various reaction conditions may be calculated and are listed in Table 1.

Consistent with the results in Fig. 2, the data in Table 1 show that the rate of disappearance of $[Fe_3(CO)_{12}]$ is independent of its concentration. However, the rate exhibits a first-order dependence in the concentration of PPh_3. A plot of the rate *vs.* $[PPh_3]$ is linear with a slope of (2.34 ± 0.05) × 10^{-5} s^{-1} and a y intercept of virtually zero (Fig. 3). The slope and the standard deviation were estimated by the method of least squares. Consequently, the rate for reaction (3) may be expressed as in equation (4) where $k' = (2.34 \pm 0.05) \times 10^{-5}$ s^{-1} at 20 °C.

$$d[Fe_3(CO)_{12}]/dt = k'[PPh_3] \quad (4)$$

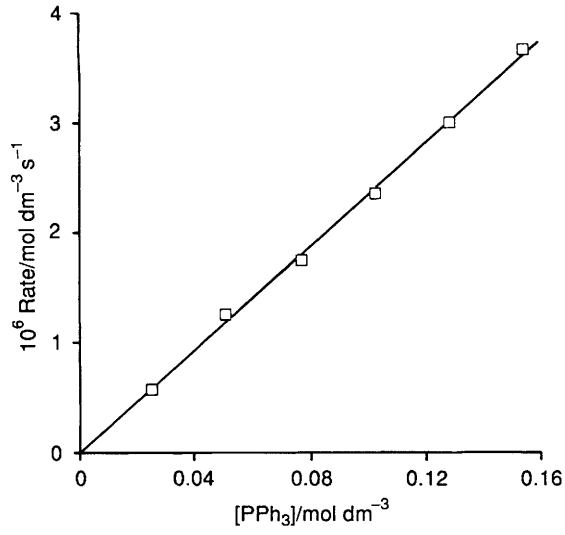

Fig. 3 Effect of the concentration of PPh_3 on the substitution rate of $[Fe_3(CO)_{12}]$ [(2.49 ± 0.05) × 10^{-3} mol dm^{-3}]; runs 1–6

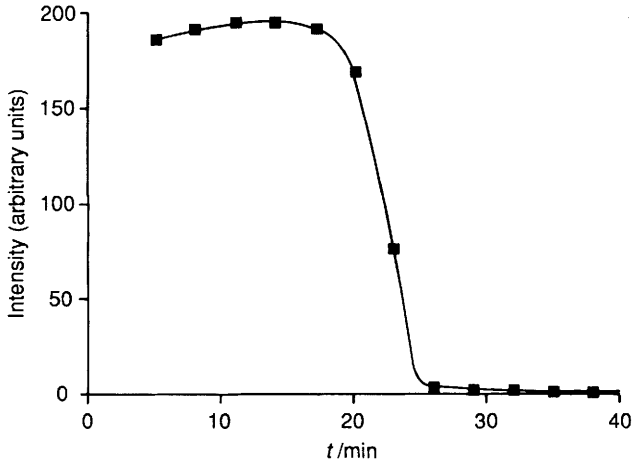

Fig. 4 The intensity of the $[Fe_3(CO)_{12}]^{\bullet -}$ signal as a function of time; $[Fe_3(CO)_{12}]$ = 5.02 × 10^{-3}, $[PPh_3]$ = 1.57 × 10^{-1} mol dm^{-3}, 20 ± 0.5 °C. The concentration of $[Fe_3(CO)_{12}]^{\bullet -}$ at maximum intensity is estimated to be 1.5 × 10^{-3} mol dm^{-3}

It is notable that the reaction of $[Fe_3(CO)_{12}]$ with PPh_3 in thf is very sensitive to how these reactants and solvent are prepared and stored. Aged thf and $[Fe_3(CO)_{12}]$ generally lead to slower reaction rates and a longer induction period. In these kinetic runs the $[Fe_3(CO)_{12}]$ used was freshly prepared and was stored at −10 °C under argon. The addition of 0.1 equivalent of the one-electron oxidant $[Fe(\eta\text{-}C_5H_5)_2][PF_6]$ to a thf reaction solution greatly inhibits the substitution. The observed solvent dependence of the substitution rate is similar to that for the reaction of $[Fe_3(CO)_{12}]$ with CO.[17] Consequently, it is likely that the PPh_3 substitution also follows an electron-transfer-catalysed mechanism.

EPR Study.—Evidence for the presence of odd-electron iron carbonyl anions was obtained by measuring the EPR spectra of the reacting solutions. A singlet signal at g = 2.0018 was detected at 20 °C in the thf solutions of $[Fe_3(CO)_{12}]$ and PPh_3. The radical may be observed over the temperature range −80 to 30 °C and is the 19-electron iron carbonyl anion $[Fe_3(CO)_{12}]^{\bullet -}$. Its structure has been assigned by Krusic *et al.*[23] using an isotopic labelling method. Although they observed the signal of $[Fe_3(CO)_{12}]^{\bullet -}$ at −80 °C, we have found that the radical also may be detected at room temperature. In some cases, two weak signals at g = 2.0474 (t, a = 25.0) and 2.0487 (d, a = 21.8 G) were also observed. There is still no report in the literature concerning these two EPR signals. However, it is clear from their splitting patterns that one and two PPh_3 are co-ordinated to the metal centre of the doublet and triplet radicals respectively. The intensity of the $[Fe_3(CO)_{12}]^{\bullet -}$ signal exhibits an intriguing variation with reaction time, as shown in Fig. 4. In the time interval 4–20 min the intensity changes only slightly and may be considered to be constant. Because it takes *ca.* 2 min to dissolve $[Fe_3(CO)_{12}]$ and PPh_3 in thf, the intensity of the EPR signal during this initial period could not be directly measured. A rapid increase in intensity of the $[Fe_3(CO)_{12}]^{\bullet -}$ signal is expected within this period. As the reaction proceeds for *ca.* 20 min the $[Fe_3(CO)_{12}]^{\bullet -}$ signal started to drop sharply to a value of < 3% of the maximum intensity. A comparison of the results of ultraviolet–visible and EPR studies indicates that as the concentration of $[Fe_3(CO)_{12}]^{\bullet -}$ started to decrease sharply the conversion of $[Fe_3(CO)_{12}]$ into $[Fe_3(CO)_{11}(PPh_3)]$ was nearly complete.

The concentration of the radical anion $[Fe_3(CO)_{12}]^{\bullet -}$ exhibits an interesting dependence on $[Fe_3(CO)_{12}]$ and $[PPh_3]$. As shown in Fig. 5, a plot of the intensity of the $[Fe_3(CO)_{12}]^{\bullet -}$ signal *vs.* $[PPh_3]$ yields a straight line of zero y intercept indicative of a first-order dependence of $[Fe_3(CO)_{12}^{\bullet -}]$ on $[PPh_3]$. By using dpph as an external standard, the concentration of $[Fe_3(CO)_{12}]^{\bullet -}$ may be estimated. At the relative intensity of $[Fe_3(CO)_{12}]^{\bullet -}$ = 1 in Fig. 5 the corresponding concentration of $[Fe_3(CO)_{12}]^{\bullet -}$ is 1.2 × 10^{-3} mol dm^{-3}. Thus, the relation in Fig. 5 may be expressed by equation (5) where k'' = 8.7 × 10^{-3}. On the other

$$[Fe_3(CO)_{12}^{\bullet -}] = k''[PPh_3] \quad (5)$$

hand, a plot of the same intensity against the initial concentration of $[Fe_3(CO)_{12}]$ is linear with zero slope within experimental error, revealing independence of $[Fe_3(CO)_{12}]$ (see Table 1, runs 3 and 7–9). On the basis of the relation in Fig. 5, equation (4) may be rewritten as (6) with k = (2.7 ± 0.1) × 10^{-3}

$$d[Fe_3(CO)_{12}]/dt = k'[PPh_3] = (k'/k'')[Fe_3(CO)_{12}^{\bullet -}] = k[Fe_3(CO)_{12}^{\bullet -}] \quad (6)$$

s^{-1}. Thus, it is apparent that the substitution rate of reaction (3) is first order in the concentration of $[Fe_3(CO)_{12}]^{\bullet -}$. The close relation of substitution rate to the concentration of $[Fe_3(CO)_{12}]^{\bullet -}$ is further supported by the following observations. First, both the substitution rate and the concentration of $[Fe_3(CO)_{12}]^{\bullet -}$ are independent of the concentration of $[Fe_3(CO)_{12}]$. Secondly, the EPR signal of $[Fe_3(CO)_{12}]^{\bullet -}$ essentially disappeared on addition of the electron acceptor $[Fe(\eta\text{-}C_5H_5)_2]^+$ to a thf solution of $[Fe_3(CO)_{12}]$ and PPh_3 and the rate of substitution was also strongly inhibited by the presence of the same cation.

Mechanism.—In view of the correlation between the concentration of $[Fe_3(CO)_{12}]^{\bullet -}$ and the rate of reaction (3), it is reasonable to assume that $[Fe_3(CO)_{12}]^{\bullet -}$ is the active species responsible for the substitution. An electron-transfer-catalysed process as shown in Scheme 1 is proposed to account for the reaction. In the mechanism the 19-electron $[Fe_3(CO)_{12}]^{\bullet -}$ radical first dissociates a CO ligand to give $[Fe_3(CO)_{11}]^{\bullet -}$. This 17-electron species then picks up a PPh_3 ligand to yield $[Fe_3(CO)_{11}(PPh_3)]^{\bullet -}$. Finally, the extra electron in $[Fe_3(CO)_{11}(PPh_3)]^{\bullet -}$ is transferred to $[Fe_3(CO)_{12}]$ regenerating $[Fe_3(CO)_{12}]^{\bullet -}$. From the results of the kinetic studies that the rate of reaction depends only on the concentration of $[Fe_3(CO)_{12}]^{\bullet -}$, the CO dissociation of $[Fe_3(CO)_{12}]^{\bullet -}$ to give $[Fe_3(CO)_{11}]^{\bullet -}$ should be the rate-limiting step for the observed electron catalysis. Thus the rate constant k in equation (6) for the observed catalysis is also a measure of the CO dissociation rate of $[Fe_3(CO)_{12}]^{\bullet -}$. To the best of our knowledge, this is the

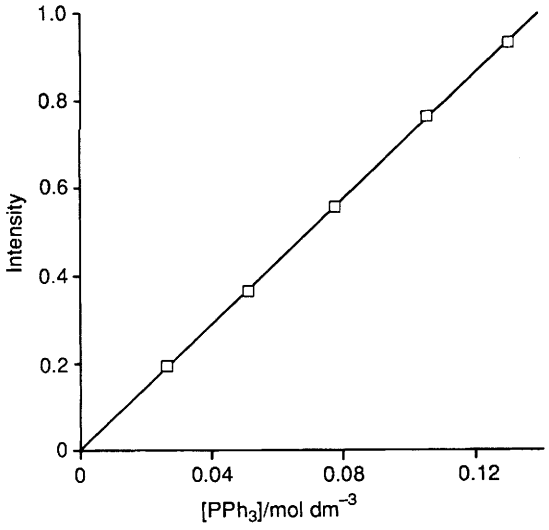

Fig. 5 The maximum EPR intensity of $[Fe_3(CO)_{12}]^{\bullet-}$ as a function of the concentration of PPh_3. The concentration of $[Fe_3(CO)_{12}]^{\bullet-}$ is estimated to be 1.2×10^{-3} mol dm^{-3} at the relative intensity 1; $[Fe_3(CO)_{12}] = 2.66 \times 10^{-3}$ mol dm^{-3}, 20 ± 0.5 °C

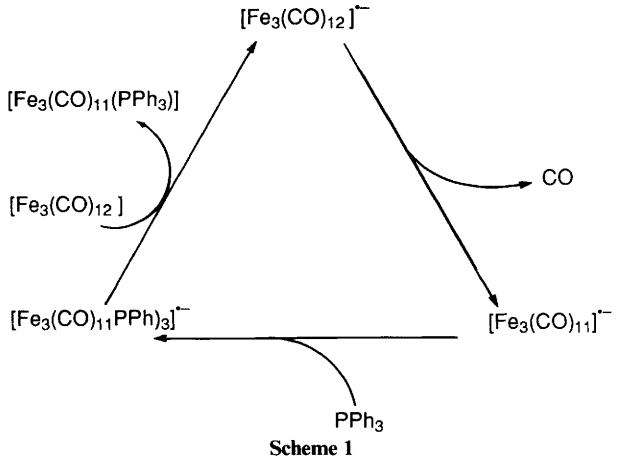

Scheme 1

only rate constant obtained for the dissociation of a 19-electron radical. Both the reaction of $[Fe_3(CO)_{11}]^{\bullet-}$ with PPh_3 and the electron-transfer step in Scheme 1 are relatively rapid compared to the dissociation of CO from $[Fe_3(CO)_{12}]^{\bullet-}$.

The proposed mechanism is in agreement with the observation that generally the substitution reaction of a 19-electron complex occurs *via* a dissociative pathway,[16] that of a 17-electron system *via* an associative process.[11–15] Although no direct measurement for the electron transfer from $[Fe_3(CO)_{11}(PPh_3)]^{\bullet-}$ to $[Fe_3(CO)_{12}]$ has been made, this step is expected to be energetically favourable on the basis that PPh_3 is a stronger electron-donor ligand than is CO. The reduction potentials of $[Fe_3(CO)_{11}(PPh_3)]$ and $[Fe_3(CO)_{12}]$ in acetone were measured to be −0.48 and −0.26 V respectively.[24] These values confirm the notion that $[Fe_3(CO)_{12}]$ is a better electron acceptor than is $[Fe_3(CO)_{11}(PPh_3)]$.

In our previous report[17] we proposed that the triangular $[Fe_3(CO)_{12}]^{\bullet-}$ radical undergoes Fe–Fe bond breaking to give a 17-electron linear chain species which is a key intermediate for the fragmentation of $[Fe_3(CO)_{12}]$ to $[Fe(CO)_5]$. In the present paper, however, we propose that $[Fe_3(CO)_{12}]^{\bullet-}$ undergoes CO dissociation to account for the PPh_3 substitution. A comparison of the rate of substitution and fragmentation reveals that PPh_3 substitution is at least an order of magnitude more rapid than the Fe–Fe bond-breaking process. As indicated in the kinetic studies of PPh_3 substitution of $[Fe_3(CO)_{12}]$, the latter process may be neglected.

The observed CO dissociation and Fe–Fe bond breaking of $[Fe_3(CO)_{12}]^{\bullet-}$ may be rationalized based on the results of molecular orbital (MO) calculations which show that the lowest unoccupied molecular orbital (LUMO) of $[Fe_3(CO)_{12}]$ possesses both metal–metal and metal–CO antibonding character.[25,26] Consequently, the addition of an electron to $[Fe_3(CO)_{12}]$ to give $[Fe_3(CO)_{12}]^{\bullet-}$ should weaken both the metal–metal and metal–CO bonds and thus facilitate the breaking of either bond. Examples of other polynuclear metal carbonyls that undergo both metal–metal cleavage and ligand substitution *via* e.t.c. mechanisms are known.[1,2,27]

The surprising intensity dependence of the $[Fe_3(CO)_{12}]^{\bullet-}$ signal on the concentration of PPh_3 may be explained based on the assumption that the PPh_3 used for the present investigations contains a trace of impurity the concentration of which is proportional to that of PPh_3. This impurity reacts with $[Fe_3(CO)_{12}]$ quantitatively and rapidly compared to the substitution process to yield $[Fe_3(CO)_{12}]^{\bullet-}$. Other pathways for $[Fe_3(CO)_{12}]^{\bullet-}$ formation and destruction are relatively slow. By this means we explain why the concentration of the radical anion remains approximately constant during the period of the substitution reaction. At the end of substitution, $[Fe_3(CO)_{11}(PPh_3)]^{\bullet-}$ no longer transfers its electron to $[Fe_3(CO)_{12}]$ to regenerate $[Fe_3(CO)_{12}]^{\bullet-}$ resulting in a sharp decrease in the $[Fe_3(CO)_{12}]^{\bullet-}$ concentration and the transformation of the phosphine radical anion to other species.

In agreement with the hypothesis that $[Fe_3(CO)_{12}]^{\bullet-}$ results from the reaction of $[Fe_3(CO)_{12}]$ with an impurity in PPh_3, the use of PPh_3 freshly prepared by recrystallization in thf–ethanol under nitrogen leads to a much less rapid substitution and a weaker $[Fe_3(CO)_{12}]^{\bullet-}$ signal in the EPR spectrum. One possible impurity in PPh_3 responsible for the formation of $[Fe_3(CO)_{12}]^{\bullet-}$ is PPh_3O from oxidation of PPh_3. Evidence for the presence of a trace of PPh_3O in PPh_3 is found in the IR spectrum (KBr) of PPh_3 which exhibits a very weak absorption at 1180 cm^{-1} corresponding to ν_{PO} of PPh_3O. This band does not appear in the spectrum of PPh_3 freshly recrystallized from thf–ethanol. Indeed, the addition of PPh_3O to a mixture of $[Fe_3(CO)_{12}]$ and PPh_3 in thf greatly accelerates the PPh_3 substitution rate and the intensity of the EPR signal of $[Fe_3(CO)_{12}]^{\bullet-}$ increases with the concentration of PPh_3O.

With regard to how PPh_3O interacts with $[Fe_3(CO)_{12}]$ to yield $[Fe_3(CO)_{12}]^{\bullet-}$, it is likely that this phosphine oxide induces disproportionation of $[Fe_3(CO)_{12}]$ to give an iron(II) species and the $[Fe_3(CO)_{12}]^{\bullet-}$ radical according to equations (7) and (8). In the absence of PPh_3 the $[Fe_2(CO)_8]^{\bullet-}$ signal

$$2[Fe_3(CO)_{12}] + nPPh_3O \longrightarrow [Fe_2(CO)_8]^{\bullet-} + [Fe_3(CO)_{12}]^{\bullet-} + [Fe(OPPh_3)_n]^{2+} \quad (7)$$

$$[Fe_2(CO)_8]^{\bullet-} + 2PPh_3 + [Fe_3(CO)_{12}] \longrightarrow 2[Fe(CO)_4(PPh_3)] + [Fe_3(CO)_{12}]^{\bullet-} \quad (8)$$

($g = 2.0387$) is actually detected in addition to $[Fe_3(CO)_{12}]^{\bullet-}$ and $[Fe_3(CO)_{11}]^{\bullet-}$ (very weak) in a thf solution containing $[Fe_3(CO)_{12}]$ and PPh_3O [equation (7)], while in the presence of excess of PPh_3 the $[Fe_2(CO)_8]^{\bullet-}$ and $[Fe_3(CO)_{11}]^{\bullet-}$ disappear. Similar to the effect of PPh_3O, addition of any one of the bases L such as pyridine, bipyridine, ethylenediamine and formylpiperidine to a thf solution of $[Fe_3(CO)_{12}]$ and PPh_3 greatly enhances the rate of reaction (3) and also the intensity of the $[Fe_3(CO)_{12}]^{\bullet-}$ signal in the EPR spectrum. It is known that $[Fe_3(CO)_{12}]$ disproportionates in the presence of a Lewis base L to give $[FeL_6]^{2+}$ and an iron carbonyl dianion $[Fe_2(CO)_8]^{2-}$, $[Fe_3(CO)_{11}]^{2-}$ or $[Fe_4(CO)_{13}]^{2-}$.[28–30] In one experiment, addition of $[Fe_3(CO)_{11}]^{2-}$ $[N(PPh_3)_2^+$ as the counter cation] to $[Fe_3(CO)_{12}]$ results in the formation of $[Fe_3(CO)_{12}]^{\bullet-}$ and $[Fe_3(CO)_{11}]^{\bullet-}$ radicals in addition to others. This result indicates that the dianion readily transfers one electron to $[Fe_3(CO)_{12}]$ so as to establish an equilibrium between even- and odd-electron iron carbonyl species [equation (9)].

$$[Fe_3(CO)_{11}]^{2-} + [Fe_3(CO)_{12}] \longrightarrow [Fe_3(CO)_{11}]^{\bullet -} + [Fe_3(CO)_{12}]^{\bullet -} \quad (9)$$

Previously, we reported the observation of radical anions $[Fe_3(CO)_{12}]^{\bullet -}$, $[Fe_2(CO)_8]^{\bullet -}$ and $[Fe_3(CO)_{11}]^{\bullet -}$ when $[Fe_3(CO)_{12}]$ was dissolved in the donor solvents dimethylformamide, dimethyl sulphoxide, MeCN or thf.[17] These also may be interpreted as a consequence of $[Fe_3(CO)_{12}]$ disproportionation induced by the donor solvent.

Conclusion

The substitution of PPh_3 for CO in $[Fe_3(CO)_{12}]$ following an electron-transfer-catalysed mechanism has been demonstrated. A key intermediate is believed to be $[Fe_3(CO)_{12}]^{\bullet -}$ and its CO dissociation is the rate-limiting step for the observed catalysis. The substitution rate depends only on the concentration of $[Fe_3(CO)_{12}]^{\bullet -}$ or on that of the substrate which can lead to the disproportionation of $[Fe_3(CO)_{12}]$ and the formation of $[Fe_3(CO)_{12}]^{\bullet -}$. The dependence of the rate on the concentration of PPh_3 results from the fact that the triphenylphosphine used contains a small amount of triphenylphosphine oxide. The observed rate law for reaction (3) appears to be the first example known for an electron-transfer-catalysed substitution reaction.

References

1 G. J. Bezem, P. H. Rieger and S. Visco, *J. Chem. Soc., Chem. Commun.*, 1981, 265.
2 M. Arewgoda, P. H. Rieger, B. H. Robinson, J. Simpson and S. J. Visco, *J. Am. Chem. Soc.*, 1982, **104**, 5633.
3 M. Arewgoda, B. H. Robinson and J. Simpson, *J. Am. Chem. Soc.*, 1983, **105**, 1893.
4 B. M. Peake, P. H. Rieger, B. H. Robinson and J. Simpson, *J. Am. Chem. Soc.*, 1980, **102**, 156.
5 M. Arewgoda, B. H. Robinson and J. Simpson, *J. Chem. Soc., Chem. Commun.*, 1982, 284.
6 M. I. Bruce, D. C. Kehoe, J. G. Matisons, B. K. Nicholson, P. H. Rieger and M. L. Williams, *J. Chem. Soc., Chem. Commun.*, 1982, 442.
7 T. Venalainen and T. Pakkanen, *J. Organomet. Chem.*, 1984, **266**, 269.
8 M. I. Bruce, J. G. Matisons and B. K. Nicholson, *J. Organomet. Chem.*, 1983, **247**, 321.
9 M. I. Bruce, T. W. Hambley, B. K. Nicholson and M. R. Snow, *J. Organomet. Chem.*, 1982, **235**, 83.
10 J. K. Kochi, *J. Organomet. Chem.*, 1986, **300**, 139 and refs. therein.
11 Q.-Z. Shi, T. G. Richmond, W. C. Trogler and F. Basolo, *J. Am. Chem. Soc.*, 1982, **104**, 4032.
12 M. J. Therien, C. L. Ni, F. C. Anson, J. G. Osteryoung and W. C. Trogler, *J. Am. Chem. Soc.*, 1986, **108**, 4037.
13 J. W. Hershberger, R. J. Klingler and J. K. Kochi, *J. Am. Chem. Soc.*, 1983, **105**, 61.
14 P. M. Zizelman, C. Amatore and J. K. Kochi, *J. Am. Chem. Soc.*, 1984, **106**, 3771.
15 S. B. McCullen, H. W. Walker and T. L. Brown, *J. Am. Chem. Soc.*, 1982, **104**, 4007.
16 F. Mao, D. R. Tyler and D. Keszler, *J. Am. Chem. Soc.*, 1989, **111**, 130.
17 S. L. Yang, C. S. Li and C. H. Cheng, *J. Chem. Soc., Chem. Commun.*, 1987, 1872.
18 A. Shojaie and J. D. Atwood, *Organometallics*, 1985, **4**, 187.
19 R. Kumar, *J. Organomet. Chem.*, 1977, **136**, 235.
20 J. K. Shen, Y. L. Shi, Y. C. Gao, Q. Z. Shi and F. Basolo, *J. Am. Chem. Soc.*, 1988, **110**, 2414.
21 W. McFarlane and G. Wilkinson, *Inorg. Synth.*, 1966, **8**, 181.
22 R. J. Angelici and E. E. Siefert, *Inorg. Chem.*, 1966, **5**, 1457.
23 P. J. Krusic, J. S. Filippo, L. M. Daniels, R. L. Hance and B. Hutchison, *J. Am. Chem. Soc.*, 1981, **103**, 2129.
24 A. M. Bond, P. A. Dawson, B. M. Peake, B. H. Robinson and J. Simpson, *Inorg. Chem.*, 1977, **16**, 2199.
25 D. R. Tyler, R. A. Levenson and H. B. Gray, *J. Am. Chem. Soc.*, 1978, **100**, 7888.
26 D. R. Tyler and H. B. Gray, *J. Am. Chem. Soc.*, 1981, **103**, 1683.
27 S. Jensen, B. H. Robinson and J. Simpson, *J. Chem. Soc., Chem. Commun.*, 1983, 1081.
28 W. Hieber and J. G. Floss, *Chem. Ber.*, 1957, **90**, 1617.
29 W. Hieber and R. Werner, *Chem. Ber.*, 1957, **90**, 1116.
30 W. Hieber and N. Kahlen, *Chem. Ber.*, 1958, **91**, 2223.

Received 1*st March* 1991; *Paper* 1/00966D